Trends in Applied Sciences Research

ISSN 1819-3579

Academic
Journals Inc.

www.academicjournals.com

Trends in Applied Sciences Research 1 (4): 386-401, 2006
ISSN 1819-3579

A Multi-layer Cylindrical Shell Under Electro-thermo-mechanical Loads

[1]K. Jayakumar, [1]D. Yadav and [2]B. Nageswara Rao
[1]Department of Aerospace Engineering, Indian Institute of Technology,
Kanpur-208 016, India
[2]Structural Analysis and Testing Group, Vikram Sarabhai Space Centre,
Trivandrum-695 022, India

Abstract: Utilizing the stress formulation approach a closed-form solution is obtained for a long multi-layer cylindrical shell subjected to electro-thermo-mechanical loads. The present analytical solution holds good to examine the elastic behaviour of laminated composite shells with anisotropic piezoelectric layers acting as sensor and actuator under electro-thermo-mechanical loads. Standard finite elements are not adequate for modelling of the incompressible nature of the solid propellant grains in rocket motors. Utilizing MSC/MARC© software, finite element analysis has been carried out on a three-layered (solid propellant grain/insulation/metallic casing) cylindrical shell subjected to thermal and internal pressure loads. The structure is idealized using the eight node quadrilateral isoparametric Hermann element for incompressible materials like propellant grain and insulation and regular elements for casing material. The finite element analysis results are found to be in good agreement with the present closed-form solution. This analytical solution can serve as benchmark to finite element solutions. Stress analysis has also been carried out on a three-layer cylindrical shell to examine the piezoelectric effects of one of the layers as composed of piezoelectric layers

Key words: Piezoelectricity, multi-layer cylinder, electro-thermo-mechanical loads

Introduction

Piezoelectric materials have many applications in various fields such as: smart structures, electric resonators, filters, actuators, sensors and more. The electro-mechanical response of piezoelectric materials is complex as it involves a mechanical response, an electrical response and a mutual coupling between the mechanical and electrical domains. Shell type smart structures have constituted the subject of study to fairly good number of researchers in the aerospace industry (Tzou *et al*., 1989, 1991, 1992, 1994a, b). Using the first-order shear deformation theory, Miller and Abramovich (1995) have made analytical studies on thick shell having distributed self-sensing piezoelectric actuators. Cheng and Shen (1996a, 1997), Cheng *et al*. (1996b) Tarn (2002) and Jayakumar *et al*. (2006) have examined piezoelectric circular cylindrical shell problems. Smart/intelligent materials and structures refer to structures with surface-mounted or embedded sensors and actuators. Figure 1 shows a typical smart laminated cylindrical shell. In most MEMS (micro electro-mechanical systems) applications, multi-layer piezoelectric structures are being considered as thin structures and edge effects are neglected. Paul (1966) and Paul and Raju (1982) computed frequencies for solid cylinders, whereas Paul and Venkatesan (1987) have extended the analysis including hollow cylinders. Balamurugan and Narayan (2001) have carried out the coupled analysis of piezo-laminated plate and piezo-laminated curvilinear shell structures and their vibration control performance considering the random response

Corresponding Author: Dr. B. Nageswara Rao, Structural Analysis and Testing Group, Vikram Sarabhai Space Centre, Trivandrum-695 022, India Tel: 91-471-2565831 Fax: 91-471-2564181

to random input loads. Adelman and Stavsky (1973) and Adelman (1975) have considered the coupling between the constitutive relation and the charge equations of electrostatics for the analysis of laminated composite cylinders. Mitchell and Reddy (1995) have obtained a power series solution for an axisymmetric composite cylindrical truss type structure, which are radially polarised. Chen and Shen (1997) have studied linear buckling of piezoelectric circular cylindrical shells of infinite length subjected to axisymmetric external pressure and electrical field. In the solution of Bhaskar and Varadan (1993) for an n-layer cylindrical shell, the 6n boundary and interface conditions yield a system of 6n algebraic equations to determine the 6n unknown coefficients. The method becomes complex for a cylindrical with very large number of layers.

Motivated by the work of the above researchers, an attempt is made to obtain a closed-form solution for a multi-layer cylindrical shell subjected to electro-thermo-mechanical loads utilizing the stress formulation approach. In the present formulation, each layer is idealised as a single piezoelectric circular cylinder under internal and external pressure. The interface pressures in the multi-layer cylindrical shell are evaluated assuming the continuity of the displacements at the interface. From the known interface pressure values, each layer is analysed utilizing the derived closed-form solution for a single cylindrical shell. Finite element analysis results on a three-layer cylindrical shell subjected to internal pressure are found to be in good agreement with the closed-form solution. The present analytical solution can serve as benchmark to finite element solutions. The present formulation can be applied to cylindrically anisotropic materials (electro-thermo-elastic coupling). Piezoelectric effects are also examined through the stress analysis considering one of the layers as composed of piezoelectric material.

Analytical Solution for a Single-layer Piezoelectric Cylindrical Shell

An elasto-electro-thermo analysis of generalised plane-strain of a piezoelectric circular cylindrical shell (having a and b as inner and outer radii) under thermal and pressure load is presented here (Fig. 1). This corresponds to the case of rotational symmetric loading of a piezoelectric right circular cylinder of sufficiently high ratio of length to diameter to justify the assumption of plane-strain (i.e., ε_z = constant). Referred to the cylindrical (r, θ, z) coordinates, the piezoelectric material is cylindrically anisotropic of the most general kind (Nye, 1957). For mathematical simplicity, the strain-displacement relations, the equations of equilibrium, the equations of electrostatics are expressed in cylindrical coordinate system. In this system, u, v and w are the displacement components along the radial (r), circumferential (θ) and axial (z) directions of the cylindrical shell (Fig. 2). σ_r, σ_θ, σ_z, are the normal stress components, whereas $\tau_{\theta z}$, $\tau_{r\theta}$, τ_{rz}, are the transverse (shear) stress components. ε_r, ε_θ, ε_z, are the normal strain components and $\gamma_{\theta z}$, $\gamma_{r\theta}$, γ_{rz} are shear strain components. The details of stress analysis for a piezoelectric circular cylindrical shell under thermal and pressure loads are presented below.

The constitutive equations are written in the form

$$\begin{Bmatrix} \varepsilon \\ D^e \end{Bmatrix} = \begin{bmatrix} S & d^{pT} \\ d^p & \kappa \end{bmatrix} \begin{Bmatrix} \sigma \\ E \end{Bmatrix} + \begin{Bmatrix} \alpha \\ p^\sigma \end{Bmatrix} \Delta T \tag{1}$$

Where, the strain and stress components are:

$$\{\varepsilon\} = \{\varepsilon_r, \varepsilon_\theta, \varepsilon_z, \gamma_{\theta z}, \gamma_{rz}, \gamma_{r\theta}\}^T \text{ and } \{\sigma\} = \{\sigma_r, \sigma_\theta, \sigma_z, \tau_{\theta z}, \tau_{rz}, \tau_{r\theta}\}^T$$

The electric displacements and electric field components are:

$$\{D^e\} = \{D_r, D_\theta, D_z\}^T \text{ and } \{E\} = \{E_r, E_\theta, E_z\}^T$$

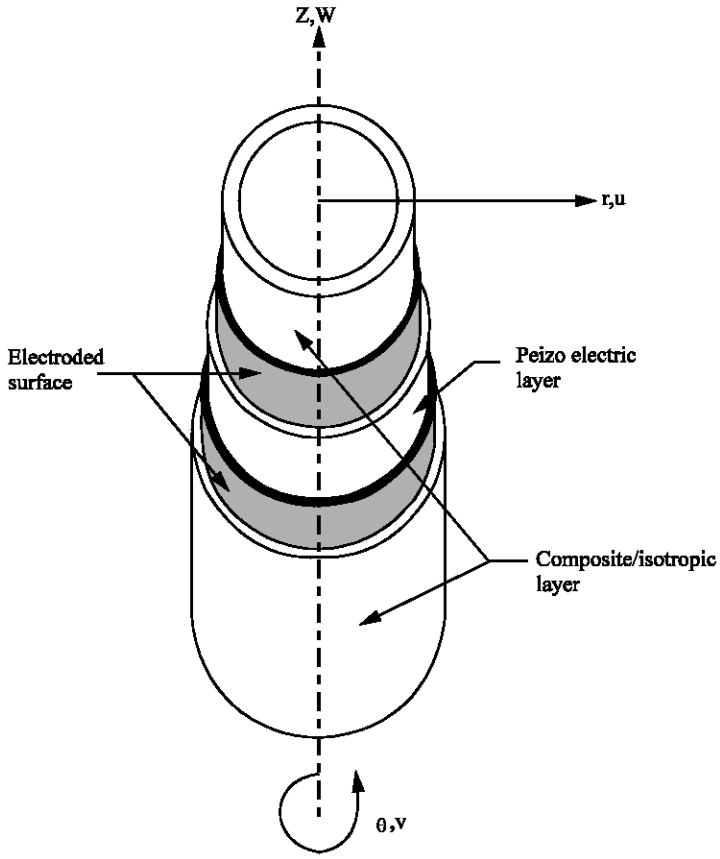

Fig. 1: A typical smart laminated cylindrical shell

The coefficients of thermal expansion measured at constant electric field and the pyroelectric coefficients measured at constant stress are $\{\alpha\} = \{\alpha_1, \alpha_2, \alpha_3, \alpha_4, \alpha_5, \alpha_6\}^T$ and $\{p^\sigma\} = \{p^\sigma_1, p^\sigma_2, p^\sigma_3\}^T$. ΔT is the temperature change, [S] is a 6×6 elastic compliance matrix, whose elements s_{ij} are measured at a constant electric field and constant temperature. Elements d^p_{ij} in the 3×6 matrix of $[d^p]$ correspond to the coefficients of converse piezoelectric effect measured at constant temperature. Elements κ_{ij} in the 3×3 matrix of $[\kappa]$ correspond to the permittivity constants measured at constant stress and constant temperature.

For axial symmetry with $v \neq 0$, the displacement components are independent of θ and hence, the strain-displacement relations for the cylindrical shell are:

$$\left(\varepsilon_r, \varepsilon_\theta, \varepsilon_z, \gamma_{\theta z}, \gamma_{rz}, \gamma_{r\theta}\right) = \left(\frac{\partial u}{\partial r}, \frac{u}{r}, \frac{\partial w}{\partial z}, \frac{\partial v}{\partial z}, \frac{\partial w}{\partial r} + \frac{\partial u}{\partial z}, \frac{\partial v}{\partial r} - \frac{v}{r}\right) \tag{2}$$

The equations of equilibrium for the generalized plane-strain conditions in the absence of body forces are:

$$\frac{\partial\left(r\sigma_r\right)}{\partial r} - \sigma_\theta = 0 \tag{3}$$

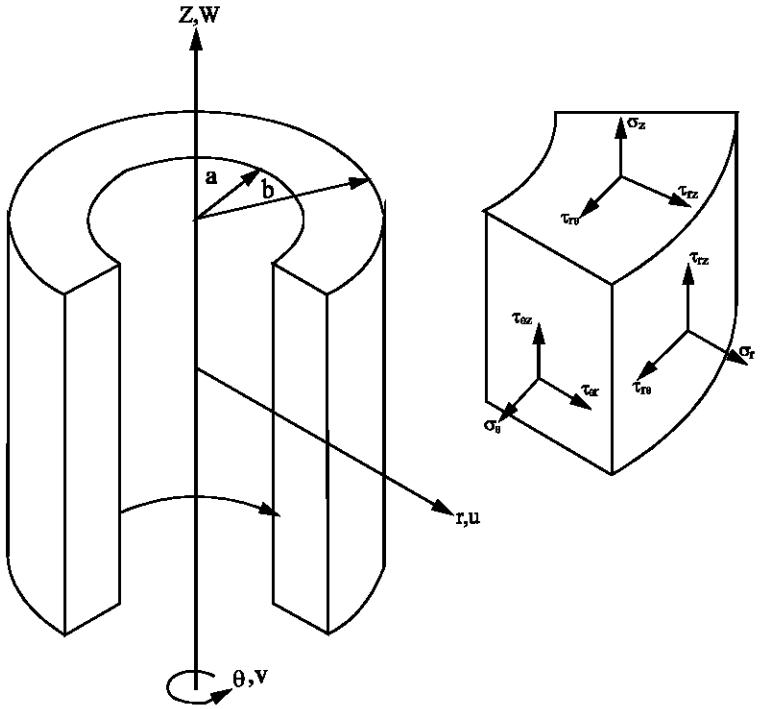

Fig. 2: Cylindrical coordinate system and six stress components on an infinitesimal volume of the axisymmetric continua

$$\frac{\partial\left(r\tau_{r\theta}\right)}{\partial r}+\tau_{r\theta}=0 \tag{4}$$

$$\frac{\partial\left(r\tau_{rz}\right)}{\partial r}=0 \tag{5}$$

The equations of electrostatics without free charges are:

$$\frac{\partial\left(rD_{r}\right)}{\partial r}=0 \tag{6}$$

The electric field components for this problem are:

$$E_{r}=-\frac{\partial\varphi}{\partial r}\ ,\ E_{\theta}=E_{z}=0 \tag{7}$$

Here, φ is the electric potential.
The solutions of Eq. (4) to (5) are:

$$\tau_{r\theta}=\frac{c_{1}}{r^{2}} \tag{8}$$

$$\tau_{rz} = \frac{c_2}{r} \tag{9}$$

$$D_r = \frac{c_3}{r} \tag{10}$$

Here, c_i's (I = 1, 2, 3) are arbitrary constants, which are to be determined from the boundary conditions.

The end conditions require that the stress resultants over the cross-section reduce to an axial force (P_z) and a torque (M_t) such that (Tarn, 2002):

$$P_z = \int_a^b (2\pi r)\sigma_z \, dr \tag{11}$$

$$M_t = \int_a^b (2\pi r) r \tau_{\theta z} \, dr \tag{12}$$

When the cylindrical shell is subjected to electromechanical loadings that do not vary axially, the resultant shear forces and moments over a cross-section, are zero identically. When the cylindrical shell is subjected to in-plane and anti-plane shears as well as uniform electric charges or voltages on the inner and outer surfaces, the boundary conditions are:

$$\tau_{r\theta} = \tau_a, \ \tau_{rz} = S_a, \ D_r = D_a \text{ or } \phi = \phi_a \qquad \text{on} \quad r = a \tag{13}$$

$$\tau_{r\theta} = \tau_b, \ \tau_{rz} = S_b, \ D_r = D_b \text{ or } \phi = \phi_b \qquad \text{on} \quad r = b \tag{14}$$

Where, the prescribed loads must satisfy the conditions: $a^2 \tau_a = b^2 \tau_b$ and $aS_a = bS_b$ for static equilibrium. Existence of an electrostatic solution requires that $aD_a = bD_b$. Hence, the arbitrary constants in Eq. 8 to 10 become:

$$c_1 = a^2\tau_a \ (\text{or} = b^2\tau_b) \tag{15}$$

$$c_2 = aS_a \ (\text{or} = bS_b) \tag{16}$$

$$c_3 = aD_a \ (\text{or} = bD_b) \tag{17}$$

From the radial component of the electric displacement (D_r) in equation (10) and the circumferential and the axial components of the electric field (E_θ and E_z) in Eq. (7), the radial component of the electric field (E_r) can be expressed in terms of stress components and the radial electric displacement (D_r) utilizing the constitutive relations (1). It is also possible to express the strain components as well as the circumferential and axial electric displacement components (D_θ and D_z) in terms of the stress components.

The stress-strain relations (1) is modified in the following form:

$$\{\varepsilon\} = [\bar{S}]\{\sigma\} + \{\alpha^*\}\Delta T + \{\beta\} D_r \tag{18}$$

Here, the elements in the 6×6 matrix of $[\bar{S}]$ are: $\bar{S}_{ij} = \bar{S}_{ij} - \beta_i d_{1j}^p$. The elements in the 6×1 matrix $\{\alpha^*\}$ are: $\alpha^*_I = \alpha_i - \beta_i p_1^{\sigma}$. The elements in the 6×1 vector of $\{\beta\}$ are: $\beta_i = \frac{d_{1i}}{\kappa_{11}}$

For simplicity Eq. 11 is rewritten in the form:

$$\begin{Bmatrix} \varepsilon_1 \\ \varepsilon_2 \end{Bmatrix} = \begin{bmatrix} A & B \\ C & D \end{bmatrix} \begin{Bmatrix} \sigma_1 \\ \sigma_2 \end{Bmatrix} \tag{19}$$

Here,

$$\{\varepsilon_1\} = \{\varepsilon_{11} - \varepsilon_{12}\} = \{\varepsilon_\theta, \varepsilon_z, \gamma_{\theta z}\}^T - \{\alpha_2^*\Delta T + \beta_2 D_r, \alpha_3^*\Delta T + \beta_3 D_r, \alpha_4^*\Delta T + \beta_4 D_r\}^T,$$

$$\{\varepsilon_2\} = \{\varepsilon_{22} - \varepsilon_{21}\} = \{\varepsilon_r, \gamma_{rz}, \gamma_{r\theta}\}^T - \{\alpha_1^*\Delta T + \beta_1 D_r, \alpha_5^*\Delta T + \beta_5 D_r, \alpha_6^*\Delta T + \beta_6 D_r\}^T,$$

$$\{\sigma_1\} = \{\sigma_\theta, \sigma_z, \tau_{\theta z}\}^T \text{ and } \{\sigma_2\} = \{\sigma_r, \tau_{rz}, \tau_{r\theta}\}^T$$

Proper care is taken while arranging the elements of the 6×6 matrix of $[\bar{S}]$ to define the elements a_{ij}, b_{ij}, c_{ij} and d_{ij} in the 3×3 matrices of A, B, C and D. Since, the stress components and for the problem under consideration is known from Eq. 8 and 9, the stress-strain relation (19) is further modified to:

$$\begin{Bmatrix} \sigma_1 \\ \varepsilon_{22} \end{Bmatrix} = \begin{bmatrix} A^* & B^* \\ C^* & D^* \end{bmatrix} \begin{Bmatrix} \varepsilon_{11} \\ \sigma_2 \end{Bmatrix} + \begin{Bmatrix} E_1^* \\ E_2^* \end{Bmatrix} \tag{20}$$

Where $A^* = A^{-1}$,

$B^* = -A^{-1}B = -A^*B$,

$D^* = D - CA^{-1}B = D - C^*B$

$C^* = CA^{-1} = CA^*$

$E_2^* = \varepsilon_{21} - C^*\varepsilon_{12}$ and

$E_1^* = -A^*\varepsilon_{12}$.

For the present case of generalized plane strain condition,

$$\varepsilon_z = \gamma_{\theta z} = \tau_{rz} = \tau_{r\theta} = 0 \tag{21}$$

From Eq. 10, one can write

$$\sigma_\theta = a_{11}^*\varepsilon_\theta + b_{11}^*\sigma_r + e_{11}^* \tag{22}$$

$$\varepsilon_r = c_{11}^*\varepsilon_\theta + d_{11}^*\sigma_r + e_{21}^* \tag{23}$$

Here, $a_{11}^*, b_{11}^*, c_{11}^*$ and d_{11}^* are the elements of the matrices A^*, B^*, C^* and D^*, respectively.

$e_{11}^* = e_{11}\Delta T + e_{12} D_r$,

$e_{21}^* = e_{21}\Delta T + e_{22} D_r$,

$$e_{11} = -(a_{11}^{*}\alpha_2^{*} + a_{12}^{*}\alpha_3^{*} + a_{13}^{*}\alpha_4^{*}),$$

$$e_{12} = -(a_{11}^{*}\beta_2 + a_{12}^{*}\beta_3 + a_{13}^{*}\beta_4),$$

$$e_{21} = -(c_{11}^{*}\alpha_2^{*} + c_{12}^{*}\alpha_3^{*} + c_{13}^{*}\alpha_4^{*} - \alpha_1^{*}) \text{ and}$$

$$e_{22} = -(c_{11}^{*}\beta_2 + c_{12}^{*}\beta_3 + c_{13}^{*}\beta_4^{*} - \beta_1^{*}).$$

Using Eq. 3 for σ_θ and Eq. 2 for ε_r and ε_θ in Eq. 12 and 23, one can obtain coupled first-order differential equations for σ_r and u. After eliminating u from these differential equations, a second-order differential equation in σ_r is obtained as:

$$\frac{\partial^2(r\sigma_r)}{\partial(\ln r)^2} + L_1\frac{\partial(r\sigma_r)}{\partial(\ln r)} + L_2(r\sigma_r) = L_3\Delta T r + L_4 c_3 \tag{24}$$

The associated boundary conditions for the differential Eq. 24 are:

$$\sigma_r = -p_a \quad \text{at} \quad r = a \tag{25}$$

$$\sigma_r = -p_b \quad \text{at} \quad r = b \tag{26}$$

Here, p_a and p_b are the applied internal and external pressures, respectively. a and b, are inner and outer radii of the cylindrical shell. Other constants in Eq. 24 are:

$$L_1 = -(b_{11}^{*} + c_{11}^{*})$$

$$L_2 = b_{11}^{*}c_{11}^{*} - a_{11}^{*}d_{11}^{*}$$

$$L_3 = a_{11}^{*}e_{21} - c_{11}^{*}e_{11} + e_{11} \text{ and}$$

$$L_4 = a_{11}^{*}e_{22} - c_{11}^{*}e_{12}.$$

The solution of Eq. 24 to 26 can be written in the form:

$$\sigma_r = A_1 r^{m_1 - 1} + A_2 r^{m_2 - 1} + (\eta_1 + \eta_3 \ln r)\Delta T + \eta_2\frac{c_3}{r} \tag{27}$$

Where,

$$A_1 = \frac{a^{m_2}A_4 - b^{m_2}A_3}{a^{m_1}b^{m_2} - a^{m_2}b^{m_1}},$$

$$A_2 = \frac{b^{m_1}A_3 - a^{m_1}A_4}{a^{m_1}b^{m_2} - a^{m_2}b^{m_1}},$$

$$A_3 = (\eta_1 + \eta_3 \ln a)(a\,\Delta T) + \eta_2 c_3 + a p_a,$$

$$A_4 = (\eta_1 + \eta_3 \ln b)(b\,\Delta T) + \eta_2 c_3 + b p_b \text{ and}$$

$$\eta_2 = \frac{L_4}{L_2}$$

m_1 and m_2 are the roots of the characteristic equation: $m^2 + L\,m + L \neq 0$. If the roots of the characteristic equation are not equal to unity, then $\eta_1 = \frac{L_3}{1+L_1+L_2}$ and $\eta_3 = 0$. Otherwise $\eta_1 = 0$ and $\eta_3 = \frac{L_3}{2+L_1}$.

After determining the radial stress component (σ_r), σ_θ is obtained directly from the equilibrium Eq. 3. The circumferential strain (ε_θ) can be obtained from Eq. 22. Using the strain-displacement relation (2) for ε_θ, the radial displacement u is determined. All other stress and strain components can be obtained directly from the modified stress-strain relation (20). From the known stresses and strains, the radial component of the electric field (E_r) can be evaluated for the specified constant $c_3 (\equiv aD_a = bD_b)$ to the radial electric displacement (D_r) in Eq. 10. The circumferential and the axial electric displacement components (D_θ, D_z) can be evaluated directly from the constitutive relation (1). Since, the radial component of the electric field (E_r) is a function of stress components and the radial electric displacement (D_r), the potential difference $\Delta\phi (\equiv \phi_a - \phi_b)$, can be worked out by integrating E_r with respect to r from r = a to r = b. Here ϕ_a and ϕ_b are the electrical potentials at inner (r = a) and outer (r = b) surfaces of cylindrical shell.

The stress and strain components are independent of z in generalized plane-strain and torsion. From the strain-displacement relation (2), the displacement components are found to be dependent on z, which can be expressed in the form:

$$u = r\varepsilon_\theta = f_u \tag{28}$$

$$v = f_v + \Theta r z + \omega r \tag{29}$$

$$w = f_w + \varepsilon_{z0} z + w_0 \tag{30}$$

Here, f_u, f_v, f_w are functions of r alone. Θ, is the twisting angle per unit length of the cylindrical shell. ω, is the rigid-body rotation about the z-axis. The constant, ε_{z0} corresponds to uniform extension and w_0 is the rigid-body displacement. In the present study, evaluation of radial displacement (u) is essential to understand the deformation pattern of a piezoelectric cylindrical shell under thermal and pressure loads.

Evaluation of Interface Pressures in a Multi-layered Cylindrical Shell

The formulation and solution developed in the preceding section for a single-layer circular cylindrical shell can be easily extended to the shells composed of multiple layers after evaluating the interface pressures assuming the radial displacement continuity at each interface.

The multi-layer cylindrical shell is composed of n co-axial cylindrical shells. For i^{th} cylinder the inner and outer radii are denoted by R_i and R_{i+1}, respectively. The interface pressures P_i and P_{i+1} acting on this cylinder are specified as the inner and outer surface pressures. The radial displacement for the i^{th} cylinder at the outer surface u_i(at $r = R_{i+1}$) is expressed as a function of R_i, R_{i+1}, P_i, P_{i+1} and the respective material properties as well as the temperature change and applied charge. Similarly, the radial displacement for the $(I + 1)^{th}$ cylinder at the inner surface u_{i+1} (at $r = R_{i+1}$) is expressed as a function of R_{i+1}, R_{i+2}, P_{i+1}, P_{i+2} and the respective material properties, temperature change and applied electric charge.

At the interface of the cylinders (at $r = R_{i+1}$), this condition provides the relation for unknown interface pressures as:

$$a_{i+1,i} P_i + a_{i+1,i+1} P_{i+1} + a_{i+1,i+2} P_{i+2} = b_{i+1} \tag{31}$$

Where, $a_{i+1,i}$, $a_{i+1, I+1}$, $a_{i+1,i+2}$ and b_{i+1} are known constants in terms of the geometric and material properties of the i^{th} and $(I + 1)^{th}$ cylinders. By substituting I = 1, 2, 3..., (n – 1) in Eq. (31) one can get interface relations for unknown interface pressures at $r = R_2, R_3,..., R_n$. It should be noted that the applied internal pressure ($P_1 = P_{internal}$) is at the inner surface ($r = R_1$) of the multi-layer cylindrical shell and the applied external pressure ($P_{n+1} = P_{external}$) is at the outer surface ($r = R_{n+1}$) of the multi-layer cylindrical shell.

The interface pressures $P_2, P_3,..., P_n$ are evaluated by solving the matrix equation:

$$\left[a_{ij}\right]\left\{P_j\right\} = \left\{b_j\right\} \qquad i, j = 1, 2, ..., (n+1) \tag{32}$$

Where, the size of the tri-diagonal square matrix $\lfloor a_{ij} \rfloor$ is (n+1) x (n+1). Size of column matrices $\{P_j\}$ and $\{b_j\}$ is (n+1)×1.

After determining P_j's (I = 1, 2, ..., (n+1)) from Eq. 32 for the applied internal and external pressures and also for the uniform temperature change (ΔT) and applied surface charge, the stress, strains and the radial displacements can be determined from the derived solution in section-2 for a single piezoelectric cylindrical shell.

Results and Discussion

The solution of the problem is examined by considering the test data on rocket motors, whose casings are made of metallic/composite materials. It is further verified by the finite element analysis of the cylindrical shell portion of a solid rocket motor composed of solid propellant grain followed by insulation and metallic casing (Fig. 3). Finally, the effect of piezoelectric response is examined for a multi-layer cylindrical shell subjected to electro-thermo-mechanical loads.

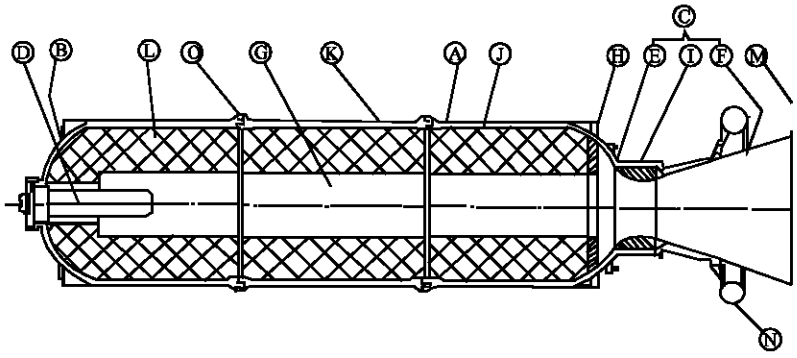

Fig. 3: Cross-section of a typical rocket motor. A) Chamber; B) Head end dome; C) Nozzle; D) Igniter; E) Nozzle convergent portion; F) Nozzle divergent portion; G) Port; H) Inhibitor; I) Nozzle throat insert; J) Lining; K) Insulation; L) Propellant; M) Nozzle exit plane; N) SITVC system; O) Segment joint

Table 1: Experimental stress analysis and comparison of analytical results on the hydro-burst pressure tested AFNOR 15CDV6 steel rocket motor case

Inner radius, R_i = 103.3 mm; Outer radius, R_O = 105.9 mm
Young's modulus, E = 203.558 GPa; Poisson's ratio, ν = 0.3
Ultimate tensile strength, σ_{ULT} = 1030 MPa; 0.2% of proof stress, σ_{YS} = 915 MPa.
The stress-strain curve is represented by:

$$\sigma = E\varepsilon\left\{1+\left(\frac{\varepsilon}{\varepsilon_0}\right)^n\right\}^{\frac{-1}{n}}$$ where ε_o = 0.005 and n = 3.2825.

Actual burst pressure of two rocket motors (Beena *et al*., 1995): 28.86 MPa, 29.59 MPa.

(a) Experimental stress analysis

Pressure (Mpa)	Strain (μ) ε_θ	Strain (μ) ε_z	Strain (μ) Effective	Effective stress (Mpa)	Modulus (Gpa)	Poisson's ratio ν	Stress (Mpa) σ_θ	Stress (Mpa) σ_z
7.75	1316	360	1357	275.1	202.7	0.301	317.5	168.5
25.51	4670	1086	4922	817.5	166.1	0.337	943.5	498.1
27.88	14778	1075	16365	1011.5	61.8	0.439	1168	579.5

(b) Comparison of analytical and experimental results

Pressure (MPa)	Hoop stress σ_θ (Mpa)	Meridional stress σ_z (MPa) $\varepsilon_z = 0$	Meridional stress σ_z (MPa) $\varepsilon_z \neq 0$ $\sigma_z(\varepsilon_z = 0) + E\varepsilon_z$	Hoop strains ε_θ (μ)
7.75	304.09	91.228	164.2	1365.1
	(317.5)+		(168.5)	(1316)
25.51	1000.9	337.11	517.49	5342.7
	(943.5)		(498.1)	(4670)
27.88	1093.9	480.24	546.68	14287
	(1168)		(579.5)	(14778)

+Results in parenthesis corresponds to test results

A comparative study is made considering test data on rocket motors (Beena *et al*., 1995), whose casing is made of AFNOR 15CDV6 steel. The pressure chambers of these motors, having diameter about 200 mm were fabricated and hydro-burst pressure tested. Since, the cylindrical portion of the motor is known to be stressed maximum under internal pressure strain gauges are mounted mostly in that portion. Using the stress-strain data from the tensile tests, stresses induced in the motor case at various pressure levels are computed for the recorded strains. Stress analysis has been carried out using the properties of the material given in Table 1. Comparison of analytical and experimental results is also given in Table 1. The analytical results of hoop stress (σ_θ) and hoop strain (ε_θ) are found to reasonably in good agreement with test results. The discrepancy in the results of meridional (σ_z) is mainly due to the assumption on the meridional strain (ε_z) assumed as zero in the present analytical solution, which is valid for cylindrical vessels having large length to diameter ratio. The measured longitudinal strains (ε_z) in the cylindrical portion of the rocket motor case presented in Table 1 were non-zero values. To bridge the gap between the present analytical solution and the measured values, a value of E ε_z is superimposed to the meridional stress (σ_z). With this the meridional stress (σ_z) values are reasonably in good agreement with test results. The failure pressure estimates of the rocket motors using the Faupel's formula:

$$P_{burst} = \frac{2}{\sqrt{3}}\sigma_{YS}\left(2-\frac{\sigma_{YS}}{\sigma_{ULT}}\right)\ln\left(\frac{R_o}{R_i}\right) = 29.20\text{MPa} \quad (33)$$

This is close to the actual burst pressure values (28.86 and 29.59 MPa) of the two rocket motors. The rocket motors after the burst test are shown in Fig. 4.

Fig. 4: AFNOR 15CDV6 steel rocket motors after the hydro-burst test (Beena *et al.*, 1995)

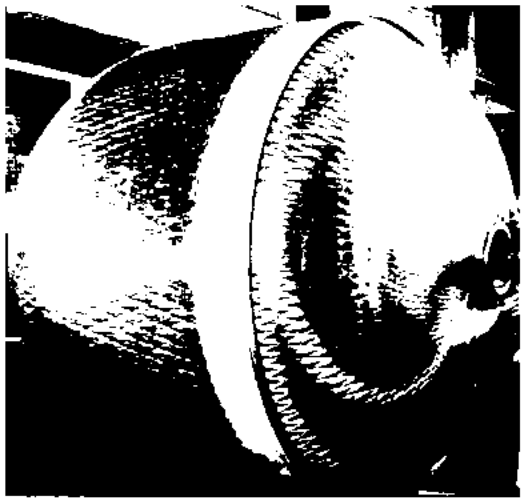

Fig. 5: A typical composite motor case

To have low mass in upper stage systems for enhancement of payload capacity of launch vehicles, upper stage rocket motors having casing made of composite materials have been designed. Strains and displacements on the outer surface of the casing were measured during proof-pressure tests. From the overall orthotropic properties in the cylindrical portion of a typical composite motor case (Fig. 5), elastic compliances are determined for stress analysis to have comparison with the proof pressure test results. Appendix gives the overall orthotropic properties and the corresponding elastic compliances considered in the stress analysis of the cylindrical shell portion of the composite motor case. The inner radius of the casing is about 980 mm and the average thickness of the cylindrical shell is around 13 mm. The measured hoop strains under proof pressure of 4.905 MPa, in the cylindrical portion of composite motor casing is 12000 (μ) whereas the present analysis gives the results as 12282 (μ). The measured radial displacement is 11.5 mm, whereas the analysis result is 11.917 mm. The analytical results are found to be in good agreement with the measured values of the proof pressure test.

The solution of the multi-layer cylindrical shell problem is examined considering the cylindrical shell portion of a solid propellant rocket motor. Stress analysis has been carried out on a three-layered (solid propellant grain/insulation/metallic casing) cylindrical shell subjected to thermal loads and pressure loads. This structure is also idealized using the eight node quadrilateral, isoparametric Hermann element of MSC/MARC® for elements of incompressible materials viz., propellant grain, insulation and regular elements for the casing material. Both axisymmetric and plane strain models were used in the comparative study. Table 2 gives the material properties for the three-layers and also provides comparison of the results for the three-layered cylindrical shell under internal pressure (4.905 MPa) and thermal load (-38°C). The finite element analysis results are in good agreement with the present analysis results.

Stress analysis is performed on a three-layered cylindrical shell that has a central piezoelectric (PZT5A) layer. Properties of the materials considered in the analysis are given in the appendix. The inner and outer layers are composed of carbon-epoxy. The stress analysis results, when the cylinder

Table 2: Comparison of analytical and finite element analysis results of a three-layer cylindrical shell subjected to thermal and pressure loads

Inner radius of the propellant grain, R1 = 500 mm
Inner radius of the insulation, R2 = 1389 mm
Inner radius of the casing, R3 = 1394 mm
Outer radius of the casing, R4 = 1401.8 mm

Material properties	Young's Modulus, (Mpa)	Poisson's ratio (ν)	Coefficient of thermal expansion α(/°C)
Casing	186390	0.3	0.000011
Insulation	1.962	0.499	0.0003
Propellant			
Pressure load	4.905	0.499	0.0001
Thermal load	1.962		

Loads	Finite element results using MSC/MARC®		Present analytical solution
	Axisymmetric elements	Plane strain elements	
Pressure 4.905 MPa			
Radial displacement at inner port (mm)	26.086	26.086	25.580
Hoop strain at inner port (%)	5.1810	5.2170	5.5060
Thermal load of -38°C			
Maximum radial stress at the interface of propellant and insulation (MPa)	0.0446	0.0445	0.0457
Maximum Hoop strain at inner port (%)	3.327	3.350	3.260

Table 3: Stress analysis results for a multi-layer piezoelectric cylindrical shell subjected to internal pressure of 1MPa using the present formulation

Pressure vessel composed of Carbon epoxy-PZT5A-Carbon epoxy.
- Inner radius = 1000 mm
- Thickness of first layer of Carbon epoxy = 10 mm
- Thickness of second layer of PZT5A = 5 mm
- Thickness of third layer of Carbon epoxy = 10 mm

	Inner layer carbon-epoxy		Middle layer PZT5A		Outer layer carbon-epoxy	
Results	Inner surface	Outer surface	Inner surface	Outer surface	Inner surface	Outer surface
Radius (mm)	1000	1010	1010	1015	1015	1025
u (mm)	4.7694-2	4.6579-2	4.6579-2	4.6558-2	4.6558-2	4.5491-2
σ_r (MPa)	-1.0000	-0.5074	-0.5074	-0.4721	-0.4721	0.0
σ_θ (MPa)	49.0900	48.4240	6.6756	6.6415	48.2270	47.618
σ_z (MPa)	9.6209	9.5863	4.0676	4.0515	9.5538	9.5265
ε_r (%)	-1.1393-2	-1.0915-2	-5.2272-2	-5.0881-2	-1.0848-2	-1.0396-2
ε_θ (%)	4.7694-3	4.6118-3	4.6118-3	4.5870-3	4.5870-3	4.4382-3

The electrical potential difference across the piezoelectric layer is 582.24 Volts

Table 4: Statistical analysis results on voltage output for a multi-layer piezoelectric cylindrical shell subjected to internal pressure of 1 MPa using the present formulation

Pressure vessel composed of Carbon epoxy-PZT5A-Carbon epoxy.
- Inner radius =1000 mm
- Thickness of first layer of Carbon epoxy = 10 mm
- Thickness of second layer of PZT5A = 5 mm
- Thickness of third layer of Carbon epoxy = 10 mm

Coefficient of variation in material properties (%)	Expected value of the output potential difference (Volts)	Coefficient of variation in the output potential difference (%)
1	576.5	0.8
2	579.4	1.6
3	582.5	2.4
4	585.8	3.2
5	589.2	4.0
6	592.9	4.9
7	596.7	5.7
8	600.8	6.6
9	605.1	7.5
10	609.6	8.3

is subjected to internal pressure of 1 MPa are given in Table 3. The electrical potential difference across the thickness of the piezoelectric layer is 582.24 Volts.

The use of probabilistic concepts to assess the reliability of structures, require the knowledge about the statistical scatter of parameters used in the models. In the design process it is rarely the case that only one variable parameter is of interest. It is with the combinations of many variable parameters that we must deal. Statistical analysis has been carried out considering a three-layer cylindrical shell that has central piezoelectric (PZT5A) layer. Material properties for carbon/epoxy and PZT5A, given in the Appendix are assumed as mean values in the present statistical analysis. Table 4 gives the dimensions of the three-layer cylindrical shell.

For the present problem, the electric potential difference $\Delta\phi(\equiv \phi_a - \phi_b)$ is functionally related to the material properties $\{S_{ij}, d_{ij}^p, \kappa_{ij}, \alpha_i, p_i^\sigma\}$ as well as the specified change in temperature (ΔT), electric displacement (D_a) and internal pressure (p_a) and external pressure (p_b). The temperature change, electric displacements, internal pressure and external pressure specified from Table 3 while evaluating $\Delta\phi$ are:

$$\Delta T = 5°C,\ p_a = 0.5074\ \text{Mpa} \quad \text{and} \quad p_b = 0.4721\ \text{MPa}.$$

Appendix

Material Properties

Composite motor casing

The overall orthotropic properties in the cylindrical shell region of the composite motor casing are:

$E_{rr} = 4.336$ GPa; $E_{\theta\theta} = 38.2904$ GPa; $E_{zz} = 23.354$ GPa; $G_{\theta z} = 2.958$ Gpa;
$G_{r\theta} = 1.054$ GPa; $\nu_{\theta z} = 0.2478$; $\nu_{rz} = 0.1014$; $\nu_{r\theta} = 0.0612$;
$\nu_{z\theta} = 0.1511$; $\nu_{zr} = 0.546$; $\nu_{\theta r} = 0.5404$; $\alpha_{rr} = 6.44\times10^{-5}/°C$; $\alpha_{\theta\theta} = -4\times10^{-7}/°C$;
$\alpha_{zz} = 2\times10^{-6}/°C$.

Compliances:

$S_{11} = 2262.443\times10^{-6}$ m^2/N; $S_{22} = 256.2\times10^{-6}$ m^2/N; $S_{33} = 420.062\times10^{-6}$ m^2/N;
$S_{44} = 3316.75\times10^{-6}$ m^2/N; $S_{55} = 9551.098\times10^{-6}$ m^2/N; $S_{66} = 9310.987\times10^{-6}$ m^2/N.
$S_{12} = -138.462\times10^{-6}$ m^2/N; $S_{13} = -229.344\times10^{-6}$ m^2/N; $S_{23} = -63.486\times10^{-6}$ m^2/N.
$S_{21} = S_{12}$; $S_{31} = S_{13}$; $S_{23} = S_{32}$.

Poisson's ratio and coefficient of thermal expansion:

$\nu_{12} = 0.612$; $\nu_{12} = 0.5404$; $\nu_{23} = 0.2478$; $\nu_{32} = 0.1511$; $\nu_{13} = 0.1014$; $\nu_{31} = 0.546$;
$\alpha_{11} = 6.44\times10^{-5}/°C$; $\alpha_{22} = -4.0\times10^{-7}/°C$; $\alpha_{33} = 2.0\times10^{-6}/°C$.

Carbon-Epoxy

Compliances:

$S_{11} = 7.0423\times10^{-12}$ m^2/N; $S_{22} = 0.9709\times10^{-12}$ m^2/N; $S_{33} = 0.9707\times10^{-12}$ m^2/N;
$S_{44} = 0.0233\times10^{-12}$ m^2/N; $S_{55} = 0.0139\times10^{-12}$ m^2/N; $S_{12} = -1.9014\times10^{-12}$ m^2/N;
$S_{13} = -1.4085\times10^{-12}$ m^2/N; $S_{12} = S_{21}$; $S_{13} = S_{31}$; $S_{23} = S_{32}$; $S_{55} = S_{66}$.

Coefficient of thermal expansion:

$\alpha_{11} = -0.9\times10^{-6}/°C$; $\alpha_{22} = 27\times10^{-6}/°C$; $\alpha_{33} = \alpha_{22}$.

Piezoelectric material PZT5A

Compliances:

$S_{11} = 16.5\times10^{-12}$ m^2/N; $S_{12} = -4.78\times10^{-12}$ m^2/N; $S_{13} = -8.45\times10^{-12}$ m^2/N;
$S_{33} = 20.70\times10^{-12}$ m^2/N; $S_{44} = 43.50\times10^{-12}$; $S_{22} = S_{11}$; $S_{12} = S_{21}$; $S_{31} = S_{13}$; $S_{23} = S_{32}$.
$S_{54} = S_{44}$; $S_{66} = 2(S_{11} - S_{12})$.

Piezoelectric strain coefficients:

$$d_{11}^p = -2.3\text{pC/N}; d_{12}^p = -d_{11}^p; d_{14}^p = -0.67\,\text{pC/N}; d_{25}^p = -d_{14}^p; d_{26}^p = -2d_{11}^p$$

Electrical permittivity:

$\kappa_{11}/\kappa_0 = 4.52$; $\kappa_{11} = \kappa_{22}$; $\kappa_0 = 8.854\times10^{-12}$F/m.

The inner and outer radii are: a = 1.01 m and b = 1.015 m.

We perform the random analysis for the piezoelectric layer, as output voltage is our prime variable of interest. The output voltage statistics is dependent on the interfacial pressure (p_a = 0.5074 Mpa and p_b = 0.4721 MPa). The interfacial pressures developed are linearly dependent on the applied internal pressure of 1 MPa for the multi-layer cylindrical shell. For the statistical analysis, variations in material properties are only considered.

Following the multivariate concept (Haugen, 1968; Bowker and Lieberman, 1972; Jeyakumar *et al*., 2005), the expected values of the output potential difference and its coefficient of variation are presented in Table 4. The coefficient of variation in the material properties varies from 1 to 10%. From the statistical analysis it was also seen that potential difference is sensitive to the material properties S_{33}, d_{12} and κ_{11}.

Conclusions

Analytical solution is obtained for a generalized plain-strain of a multi-layer cylindrical shell subjected to electro-thermo-mechanical loads. The solution of the problem is verified by considering the test data on the rocket motors, finite element analysis results of a three-layer solid propellant rocket motor and a three-layer cylindrical shell having a central piezoelectric layer, the other layers being composed of carbon-epoxy. The electrical potential difference across the thickness of the piezoelectric layer is computed from the stress analysis results. The present analytical solution can serve as benchmark to finite element solutions.

References

Adelman, N.T. and Y. Stavsky, 1973. Vibrations of radially polarised composite piezo-ceramic cylinders and disks. J. Sound and Vibration, 43: 37-64.

Adelman, N.T., Y. Stavsky and E. Segal, 1975. Axisymmetric vibrations of radially polarised piezoelectric ceramic cylinders. J. Sound and Vibration, 38: 245-254.

Balamurugan, V. and S. Narayan, 2001. Shell finite element for smart piezoelectric composite plate/shell structures and its application to the study of active vibration control. Finite Elements in Analysis and Design, 37: 713-738.

Beena, A.P., M.K. Sundaresan and B.N. Rao, 1995. Destructive tests of 15CDV6 steel rocket motor cases and their application to lightweight design. Intl. J. Pressure Vessels and Piping, 62: 313-320.

Bhaskar, K. and T.K. Varadan, 1993. Exact elasticity solution for laminated anisotropic cylindrical shells. Trans. ASME J. Applied Mechanics, 60: 41-47.

Bowker, A.H. and G.J. Lieberman, 1972. Engineering Statistics. Prentice-Hall, Englewood Cliffs, NJ.

Cheng, C.Q. and Y.P. Shen, 1996a. Piezothermoelasticity analysis for circular cylindrical shell under the state of axisymmetric deformation. Intl. J. Eng. Sci., 34: 1585-1600.

Cheng, C.Q., Y.P. Shen and X.M. Wang, 1996b. Exact solution of orthotropic cylindrical shell with piezoelectric layers under cylindrical bending. Intl. J. Solids and Structures, 33: 4481-4494.

Cheng, C.Q. and Y.P. Shen, 1997. Stability analysis of piezoelectric circular cylindrical shells. ASME J. Applied Mechanics, 64: 847-852.

Haugen, E.B., 1968. Probabilistic Approaches to Design. John Wiley and Sons, New York.

Jayakumar, K., D. Yadav and B.N. Rao, 2006. A piezoelectric cylindrical shell under thermal and pressure loads. Trends in Applied Sci. Res., 1: 214-225.

Jeyakumar, D., K.K. Biswas and B.N. Rao, 2005. Stage separation dynamic analysis of upper stage of a multistage launch vehicle using retro rockets. Mathematical and Computer Modelling, 41: 849-866.

Miller, S.E. and H. Abramovich, 1995. A self-sensing piezo-laminated actuator model for shells using a first order shear deformation theory. J. Intelligent Material Systems and Structures, 6: 624-638.

Mitchell, J.A. and J.N. Reddy, 1995. A study of embedded piezoelectric layers in composite cylinders. J. Sound and Vibration, 62: 166-173.

Nye, J.F., 1957. Physical Properties of Crystals, Clarendon Press, Oxford.

Paul, H.S., 1966. Vibrations of circular cylindrical shells of piezoelectric silver iodide crystals. J. Acoustical Soc. Am., 40: 1077-1080.

Paul, H.S. and D.P. Raju, 1982. Asymptotic analysis of the modes of wave propagation in a piezoelectric solid cylinder. J. Acoustical Soc. Am., 71: 255-263.

Paul, H.S. and M. Venkatesan, 1987. Vibrations of a hollow circular cylinder of piezoelectric ceramics. J. Acoustical Soc. Am., 82: 952-956.

Tarn, J.Q., 2002. Exact solutions of a piezoelectric circular tube or bar under extension, torsion, pressurising, shearing, uniform electric loading and temperature change. Proceedings of the Royal Society of London, A458, pp: 2349-2367.

Tzou, H.S. and M. Gadre, 1989. Theoretical analysis of a multi-layered thin shell coupled with piezoelectric shell actuators for distributed vibration controls. J. Sound and Vibration, 132: 433-450.

Tzou, H.S. and C.L. Tseng, 1991. Distributed modal identification and vibration control of continua: Piezoelectric element formulation and analysis. Trans. ASME J. Dynamic Systems, Measurements and Control, 113: 500-505.

Tzou, H.S. and G.L. Anderson, 1992. Intelligent Structural Systems. Kluwer Academic Publishers, Dordrecht, The Netherlands.

Tzou, H.S. and R. Ye, 1994a. Piezothermoelasticity and precision control of piezoelectric systems. Trans. ASME J. Vibration and Acoustics, 116: 489-495.

Tzou, H.S., J.P. Zhong and J.J. Holkamp, 1994b. Spatially distributed orthogonal piezoelectric shell actuators: Theory and application. J. Sound and Vibration, 177: 363-378.